Applied Physics Express

The Japan Society of Applied Physics

**OPEN ACCESS**

# Annealing of an AlN buffer layer in $N_2$–CO for growth of a high-quality AlN film on sapphire

To cite this article: Hideto Miyake *et al* 2016 *Appl. Phys. Express* **9** 025501

View the article online for updates and enhancements.

## Related content

- Effects of AlN buffer layer thickness on the crystallinity and surface morphology of 10-µm-thick *a*-plane AlN films grown on *r*-plane sapphire substrates
Chia-Hung Lin, Shinya Tamaki, Yasuhiro Yamashita et al.
- Polarity control of GaN grown on pulsed-laser-deposited AlN/GaN template by metalorganic vapor phase epitaxy
Jinyeop Yoo, Kanako Shojiki, Tomoyuki Tanikawa et al.
- Effect of surface pretreatment of *r*-plane sapphire substrates on the crystal quality of *a*-plane AlN
Chia-Hung Lin, Daiki Yasui, Shinya Tamaki et al.

## Recent citations

- High-quality and highly-transparent AlN template on annealed sputter-deposited AlN buffer layer for deep ultra-violet light-emitting diodes
Chia-Yen Huang *et al*
- High quality thin AlN epilayers grown on Si(110) substrates by metal-organic chemical vapor deposition
Xu-Qiang Shen *et al*
- Effects of AlN buffer layer thickness on the crystallinity and surface morphology of 10-µm-thick *a*-plane AlN films grown on *r*-plane sapphire substrates
Chia-Hung Lin *et al*

This content was downloaded from IP address 161.139.222.41 on 07/11/2017 at 07:45

OPEN ACCESS

Applied Physics Express **9**, 025501 (2016)
http://doi.org/10.7567/APEX.9.025501

# Annealing of an AlN buffer layer in $N_2$–CO for growth of a high-quality AlN film on sapphire

Hideto Miyake[1,2]*, Gou Nishio[2], Shuhei Suzuki[2], Kazumasa Hiramatsu[2], Hiroyuki Fukuyama[3], Jesbains Kaur[4], and Noriyuki Kuwano[4]

[1] *Graduate School of Regional Innovation Studies, Mie University, Tsu 514-8507, Japan*
[2] *Department of Electrical and Electronic Engineering, Mie University, Tsu 514-8507, Japan*
[3] *Institute of Multidisciplinary Research for Advanced Materials (IMRAM), Tohoku University, Sendai 980-8577, Japan*
[4] *Malaysia-Japan International Institute of Technology (MJIIT), Universiti Teknologi Malaysia (UTM), 54100 Kuala Lumpur, Malaysia*

*E-mail: miyake@elec.mie-u.ac.jp

Received October 2, 2015; accepted December 11, 2015; published online January 6, 2016

The annealing of an AlN buffer layer in a carbon-saturated $N_2$–CO gas on a sapphire substrate was investigated. The crystal quality of the buffer layer was significantly improved by annealing at 1650–1700 °C. An AlN buffer layer with a thickness of 300 nm was grown by metalorganic vapor phase epitaxy (MOVPE), and was annealed at 1700 °C for 1 h. We fabricated a 2-µm-thick AlN layer on the annealed AlN buffer layer by MOVPE. The full widths at half maximum of the (0002)- and $(10\bar{1}2)$-plane X-ray rocking curves were 16 and 154 arcsec, respectively, and the threading dislocation density was $4.7 \times 10^8$ cm$^{-2}$. © 2016 The Japan Society of Applied Physics

AlN has attracted attention for applications in the deep-ultraviolet (UV) region because of its wide direct band gap and excellent thermal and chemical stability.[1–3] However, high-density threading dislocations exist in AlN epitaxial films owing to the large lattice and thermal mismatch between AlN and substrates such as sapphire.[4] Therefore, the control of AlN growth near the interface between the AlN and sapphire substrate is one of the most important issues in the realization of high-efficiency UV devices.[5,6] To prevent the generation of threading dislocations in the AlN epitaxial layer, the nucleation layer has been controlled.[7–12] However, the AlN crystal quality can still be improved by optimizing the nucleation conditions.

Nitridation of a sapphire surface was reported using a carbon-saturated $N_2$–CO gas mixture at a high temperature.[13,14] Additionally, in the case of GaN grown on sapphire substrates, the solid-phase epitaxy of nucleation layers, such as GaN and AlN, by annealing is commonly used to improve the crystal quality of GaN films.[15–17] However, there are only a few reports on the effects of annealing AlN buffer layers on AlN growth.

In this work, we studied the effects of annealing an AlN buffer layer in a carbon-saturated $N_2$–CO mixture on the growth of high-quality AlN on a sapphire substrate. The effects of annealing were investigated as a function of the AlN buffer layer thickness and annealing temperature.[18]

AlN epilayers were grown on *c*-plane sapphire substrates by metalorganic vapor phase epitaxy (MOVPE). Trimethylaluminum (TMAl) and ammonia ($NH_3$) were used as the Al and N precursors, respectively. Prior to the growth, the substrates were cleaned in $H_2$ ambient at $T_{Clean} = 1100$ °C for 10 min. AlN buffer layers with thicknesses of $t_{Buf} = 100$–1000 nm were grown at $T_{Buf} = 1150$–1200 °C under a pressure of 30 Torr. Subsequently, the AlN buffer layers were thermally annealed in a carbon-saturated $N_2$–CO gas mixture at 1500–1750 °C for 2 h. A graphite resistance furnace was used for the annealing experiments. Table I shows the partial pressures of $N_2$ and CO gases as a function of annealing temperature.[13,14] The flow rate of the gas mixture was 2.0 L/min during the annealing. In order to prevent desorption of the AlN layer, the partial pressure of $N_2$ was chosen to be 5–15% rich of the phase equilibrium condition of AlN+C and $Al_2O_3$+C. For annealing with partial pressures of $N_2$: 0.9 atm and CO: 0.1 atm at 1700 °C, the surface of AlN buffer layers became rough because of the $Al_2O_3$ decomposition from the interface of the AlN layer and the sapphire substrate.

**Table I.** Annealing condition of AlN buffer on sapphire using $N_2$–CO gas mixture.[14]

| Annealing temperature (°C) | Partial pressure (atm) | |
|---|---|---|
| | $N_2$ | CO |
| 1500 | 0.9 | 0.1 |
| 1550 | 0.85 | 0.15 |
| 1600 | 0.8 | 0.2 |
| 1650 | 0.7 | 0.3 |
| 1700 | 0.6 | 0.4 |
| 1750 | 0.5 | 0.5 |

Finally, high-temperature (HT) AlN layers with a thickness of $t_{HT} = 2$ µm were grown on the AlN buffer layers in a $H_2$–$N_2$ mixture at $T_{HT} = 1450$ °C under 30 Torr by the MOVPE. The growth rate of the HT-AlN layers was 1 µm/h. The crystalline quality of the AlN was characterized by X-ray diffraction analysis with asymmetric Ge(220) and symmetric Ge(440) monochromators and transmission electron microscopy (TEM), and the surface morphology was examined by atomic force microscopy (AFM).

Figure 1 shows AFM images of the AlN buffer layers with $t_{Buf} = 200$, 300, and 1000 nm grown at $T_{Buf} = 1150$ °C before and after annealing at $T_{An} = 1650$ °C. The root-mean-square (RMS) surface roughness of the AlN buffer layers increases as the thickness AlN increases. After annealing the AlN buffer layers, the surface morphologies were markedly changed, and the RMS values were improved. The surfaces of the AlN buffer layers with a thickness of 300 nm or less were smooth. In particular, the RMS value of the annealed AlN buffer layer with $t_{Buf} = 300$ nm (e) was 0.49 nm, and

Content from this work may be used under the terms of the Creative Commons Attribution 4.0 license. Any further distribution of this work must maintain attribution to the author(s) and the title of the work, journal citation and DOI.

 © 2016 The Japan Society of Applied Physics

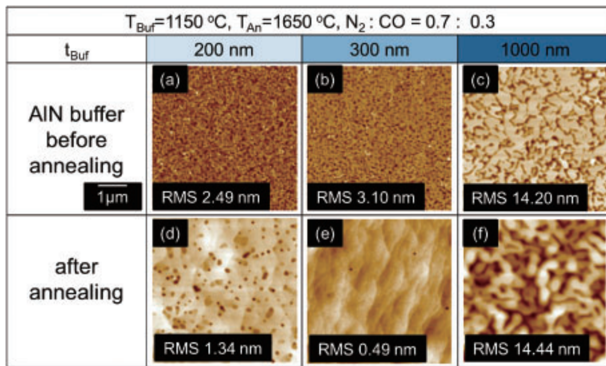


**Fig. 1.** AFM images of AlN buffer layers with various thicknesses grown at $T_{Buf}$ = 1150 °C (a–c) before and (d–f) after annealing at $T_{An}$ = 1650 °C: (a, d) $t_{Buf}$ = 200 nm, (b, e) $t_{Buf}$ = 300 nm, and (c, f) $t_{Buf}$ = 1000 nm. The scanning area in the AFM is 5 × 5 μm$^2$.

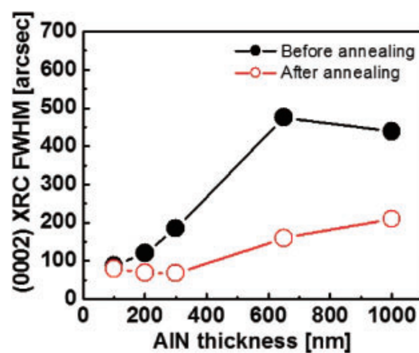


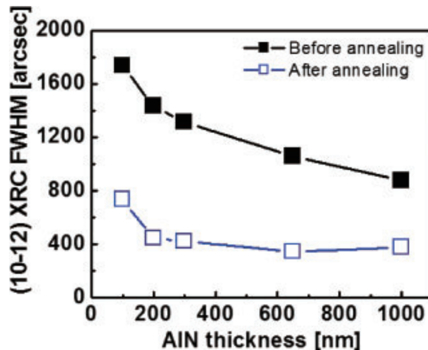


**Fig. 2.** FWHMs of (a) (0002)- and (b) (10$\bar{1}$2)-plane XRCs for AlN buffer layers with various thicknesses grown at $T_{Buf}$ = 1150 °C before and after annealing at $T_{An}$ = 1650 °C.

atomic steps were observed on its surface. However, the surface of the AlN buffer layer with $t_{Buf}$ = 1000 nm was rough even after annealing.

The full widths at half maximum (FWHMs) of the (0002)- and (10$\bar{1}$2)-plane X-ray rocking curves (XRCs) using an asymmetric Ge(220) monochromator for the AlN buffer layers with thicknesses of 100–1000 nm, which were grown at $T_{Buf}$ = 1150 °C and annealed at $T_{An}$ = 1650 °C, are shown in Figs. 2(a) and 2(b), respectively. Compared with those for the samples before annealing, the FWHMs of the XRCs for the samples after annealing were significantly decreased. This indicates that the crystalline quality of AlN was improved by annealing. The minimum FWHM of the (0002)-plane XRC was obtained in the sample with $t_{Buf}$ = 300 nm and gradually increased with increasing $t_{Buf}$. The FWHMs of the (0002)- and (10$\bar{1}$2)-plane XRCs for the sample with $t_{Buf}$ = 300 nm were 68 and 421 arcsec, respectively.

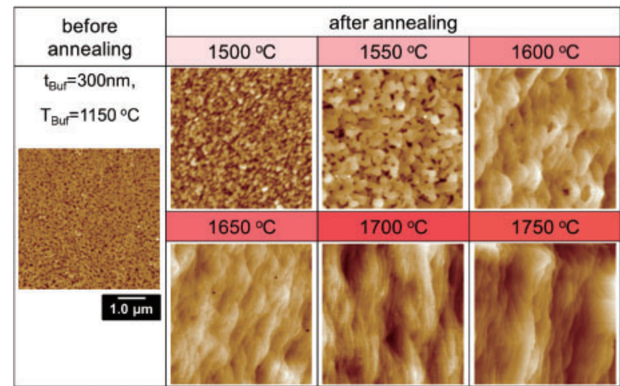


**Fig. 3.** AFM images of the AlN buffer layers with $t_{Buf}$ = 300 nm grown at $T_{Buf}$ = 1150 °C before and after annealing at $T_{An}$ = 1500–1700 °C. The scanning area in the AFM is 5 × 5 μm$^2$.

Figure 3 shows AFM images of the AlN buffer layers with $t_{Buf}$ = 300 nm grown at $T_{Buf}$ = 1150 °C before and after annealing at $T_{An}$ = 1500–1700 °C. The surface of the AlN buffer layer without annealing was observed to have small grains, and the RMS value was 3.1 nm. After annealing at temperatures above 1500 °C, the RMS value markedly decreased with increasing annealing temperature. The RMS value for the AlN buffer layers after annealing at $T_{An}$ = 1650 °C was 0.49 nm. Figure 4 shows the FWHMs of the (a) (0002)- and (b) (10$\bar{1}$2)-plane XRCs for the AlN buffer layers after annealing at various temperatures. The dotted line shows the FWHM of the XRC for the AlN buffer layer before annealing. The FWHM of the (0002)-plane XRC decreased after annealing but increased at temperatures above 1650 °C. The FWHM of the (10$\bar{1}$2) plane XRC monotonically decreased with increasing annealing temperature up to 1700 °C but increased at 1750 °C. For the AlN buffer layer annealed at 1750 °C, the FWHMs of the (0002)- and (10$\bar{1}$2)-plane XRCs increased, and the surface became rough owing to the decomposition of AlN. It was considered that the surface roughness was caused by the thermal decomposition of the AlN buffer layer during annealing. This phenomenon has also been observed in AlN films formed by the thermal nitridation of sapphire substrates.[14,19]

It was found that the mechanism of crystal quality improvement was related to solid-phase reactions at annealing temperatures of 1500–1600 °C from the AFM images shown in Fig. 3 and cross-sectional TEM observations. Figure 5 shows the TEM micrographs of the AlN buffer layer on sapphire annealed at 1500 and 1550 °C. In the AlN layer annealed at 1500 °C, inverted cone-shaped domains were observed as shown in Fig. 5(a).[9] The domains are in contact with one another. After annealing at 1550 °C, the AlN layer has changed to have a two-layer structure, as shown in Fig. 5(b). The boundary between the upper and the lower layers is rather flat in parts but bends in a zig-zag manner. It was confirmed that the zig-zag boundary propagates transversely in the whole area of the AlN layer. Evaluating the mutual similarity in the microstructures between Figs. 5(a) and 5(b), the upper layer seems to be formed by coalescence of the inverted cone-shaped domains. It is considered that


© 2016 The Japan Society of Applied Physics

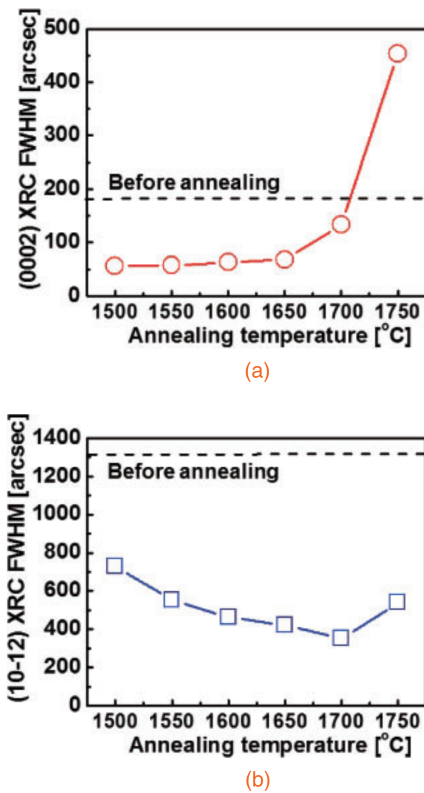


**Fig. 4.** FWHMs of (a) (0002)- and (b) $(10\bar{1}2)$-plane XRCs for AlN buffer layers with $t_{Buf} = 300$ nm grown at $T_{Buf} = 1150$ °C after annealing at various temperatures. The dotted line shows the FWHM of the XRC of the AlN buffer layer before annealing.

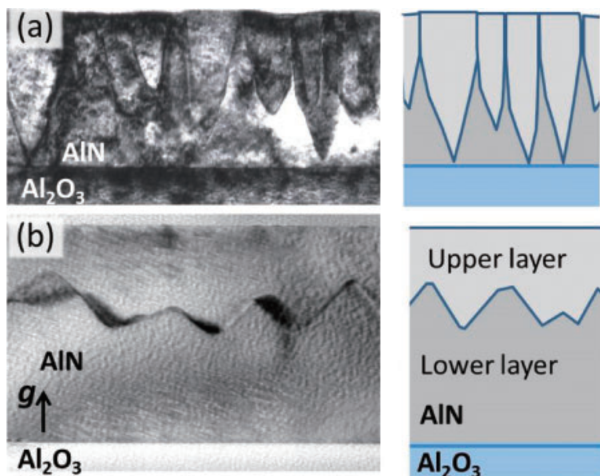


**Fig. 5.** Cross-sectional TEM images of annealed AlN buffer layers on sapphire and their schematic microstructures (a) annealed at 1500 °C, bright-field image, zone axis illumination ∥ $[2\bar{1}\bar{1}0]$; and (b) annealed at 1550 °C, bright-field-image, two-beam condition with $g = 0002$.

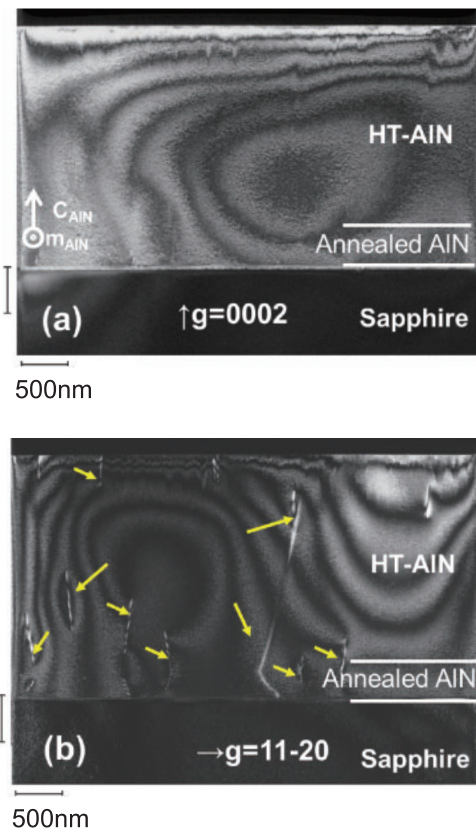


**Fig. 6.** Dark-field cross-sectional TEM images of AlN with $t_{HT} = 2$ µm grown at $T_{HT} = 1450$ °C on annealed AlN buffer layers ($T_{Buf} = 1200$ °C, $t_{Buf} = 300$ nm, $T_{An} = 1700$ °C) under the two-beam condition with (a) $g = 0002$ and (b) $g = 1\bar{1}00$. The thickness of the TEM specimen is about 100 nm. No type-***a***+***c*** or type-***c*** dislocations can be observed in (a). Type-***a*** dislocations can be observed in (b), and their density is estimated to be $5 \times 10^8$ cm$^{-2}$.

domain boundaries can be eliminated by the lateral growth and mutual coalescence of domains even if boundaries penetrate vertically up to the top surface. This finding will be reported elsewhere.

After annealing at 1700 °C for 1 h in the case of the MOVPE-grown AlN buffer layer with $t_{Buf} = 300$ nm at $T_{Buf} = 1200$ °C, we also grew an AlN film (HT-AlN) with a thickness of 2 µm on the annealed AlN buffer layer at 1450 °C by MOVPE. The FWHMs of the (0002)- and $(10\bar{1}2)$-plane XRCs using a symmetric Ge(440) monochromator were 16 and 154 arcsec, respectively. Figures 5(a) and 5(b) show dark-field cross-sectional TEM images of AlN under the two-beam condition with $g = 0002$ and $1\bar{1}00$, respectively. Threading dislocations are characterized as type-***a*** (edge type), type-***c*** (screw type), and type-***a***+***c*** (mixed type) according to their Burgers vector. Type-***c*** and type-***a***+***c*** dislocations are visible for $g = 0002$. Similarly, type-***a*** and type-***a***+***c*** dislocations are visible for $g = 1\bar{1}00$.[20] There are no dislocations in Fig. 6(a); thus, the densities of type-***c*** and type-***a***+***c*** dislocations are less than $1 \times 10^8$ cm$^{-2}$. From Fig. 6(b), the density of type-***a*** dislocations is estimated to be $5 \times 10^8$ cm$^{-2}$. We also evaluated the threading dislocation density to be $4.7 \times 10^8$ cm$^{-2}$ by observing a plan-view TEM image of the same sample. In contrast, the typical FWHM of the $(10\bar{1}2)$-plane XRC for an MOVPE-grown AlN layer on sapphire without annealing of the AlN buffer layer is 1000–2000 arcsec, and the density of type-***a*** dislocations is $10^{10}$ cm$^{-2}$.[9,21] This result indicates that the dislocations in the AlN buffer layer were annihilated by annealing.

In conclusion, we have clarified the effects of annealing in a carbon-saturated $N_2$–CO mixture on AlN buffer layers grown on sapphire substrates. The morphology and RMS value of the AlN buffer layer surface markedly changed after annealing at temperatures above 1500 °C. The FWHMs of the $(10\bar{1}2)$-plane XRCs for the AlN buffer layers significantly


© 2016 The Japan Society of Applied Physics

decreased with increasing annealing temperature up to 1700 °C. However, for the AlN buffer layers after annealing at 1750 °C, the FWHMs of the (0002)- and $(10\bar{1}2)$-plane XRCs increased and the surface was rough.

A high-quality AlN layer was successfully grown on the annealed AlN buffer layer on a sapphire substrate by MOVPE. The FWHMs of the (0002)- and $(10\bar{1}2)$-plane XRCs were 16 and 154 arcsec, respectively. Most of the threading dislocations were of type-***a***, and their density was $4.7 \times 10^8\,\text{cm}^{-2}$.

**Acknowledgments** This work was partially supported by the Akasaki Research Center of Nagoya University, Grants-in-Aid for Specially Promoted Research (No. 25000011) and Scientific Research (B) (No. 15H03556) from the Ministry of Education, Culture, Sports, Science and Technology (MEXT), the Inter-University Cooperative Research Program of the Institute for Materials Research, Tohoku University, Nanotechnology Platform Japan, Kyushu University, and Fundamental Research Grant Scheme (FRGS/2/2013/SG06/UTM/01/2) from Ministry of Education (MoE), Malaysia. This work was also funded by the Cabinet Office, Government of Japan, through its Funding Program for Next Generation World-Leading Researchers.

1) Y. Taniyasu, M. Kasu, and T. Makimoto, Nature **441**, 325 (2006).
2) Y. Taniyasu, M. Kasu, and N. Kobayashi, Appl. Phys. Lett. **81**, 1255 (2002).
3) Y. Shimahara, H. Miyake, K. Hiramatsu, F. Fukuyo, T. Okada, H. Takaoka, and H. Yoshida, Appl. Phys. Express **4**, 042103 (2011).
4) J. Bai, M. Dudley, W. H. Sun, H. M. Wang, and M. A. Khan, Appl. Phys. Lett. **88**, 051903 (2006).
5) Y. Kida, T. Shibata, H. Naoi, H. Miyake, K. Hiramatsu, and M. Tanaka, Phys. Status Solidi A **194**, 498 (2002).
6) H. Hirayama, S. Fujikawa, N. Noguchi, J. Norimatsu, T. Takano, K. Tsubaki, and N. Kamata, Phys. Status Solidi A **206**, 1176 (2009).
7) M. Imura, K. Nakano, T. Kitano, N. Fujimoto, G. Narita, N. Okada, K. Balakrishnan, M. Iwaya, S. Kamiyama, H. Amano, and I. Akasaki, Appl. Phys. Lett. **89**, 221901 (2006).
8) R. Miyagawa, S. Yang, H. Miyake, and K. Hiramatsu, Phys. Status Solidi C **8**, 2069 (2011).
9) R. Miyagawa, S. Yang, H. Miyake, K. Hiramatsu, T. Kuwahara, M. Mitsuhara, and N. Kuwano, Appl. Phys. Express **5**, 025501 (2012).
10) R. G. Banal, M. Funato, and Y. Kawakami, Appl. Phys. Lett. **92**, 241905 (2008).
11) T. Nagashima, K. Hironaka, M. Ishizuki, Y. Kumagai, A. Koukitu, and K. Takada, Phys. Status Solidi C **6**, S444 (2009).
12) Y. Ohba, H. Yoshida, and R. Sato, Jpn. J. Appl. Phys. **36**, L1565 (1997).
13) H. Fukuyama, S. Kusunoki, A. Kakomori, and K. Hiraga, J. Appl. Phys. **100**, 024905 (2006).
14) H. Fukuyama, K. Nakamura, T. Aikawa, H. Kobatake, A. Hakomori, K. Takada, and K. Hiraga, J. Appl. Phys. **107**, 043502 (2010).
15) H. Amano, N. Sawaki, I. Akasaki, and Y. Toyoda, Appl. Phys. Lett. **48**, 353 (1986).
16) S. Nakamura, Jpn. J. Appl. Phys. **30**, L1705 (1991).
17) K. Hiramatsu, S. Itoh, H. Amano, I. Akasaki, N. Kuwano, T. Shiraishi, and K. Oki, J. Cryst. Growth **115**, 628 (1991).
18) T. Nomura, K. Okumura, H. Miyake, K. Hiramatsu, O. Eryu, and Y. Yamada, J. Cryst. Growth **350**, 69 (2012).
19) Y. Kumagai, J. Tajima, M. Ishizuki, T. Nagashima, H. Murakami, K. Takada, and A. Koukitu, Appl. Phys. Express **1**, 045003 (2008).
20) F. A. Ponce, D. Cherns, W. T. Young, and J. W. Steeds, Appl. Phys. Lett. **69**, 770 (1996).
21) T. Shibata, K. Asai, S. Sumiya, M. Mouri, M. Tanaka, O. Oda, H. Katsukawa, H. Miyake, and K. Hiramatsu, Phys. Status Solidi C **0**, 2023 (2003).


© 2016 The Japan Society of Applied Physics